Carbohydrate Polymers 112 (2014) 73–76

Contents lists available at ScienceDirect

Carbohydrate Polymers

journal homepage: www.elsevier.com/locate/carbpol

Short communication

(1 → 3)-β-D-Glucan nanofibers from paramylon via electrospinning

Yutaka Kawahara[a,b,*]

[a] Division of Environmental Engineering Science, Gunma University, 1-5-1, Tenjin-cho, Kiryu 376-8515, Japan
[b] The Center for Fiber & Textile Science, Kyoto Institute of Technology, Matsugasaki, Sakyo-ku, Kyoto 606-8585, Japan

ARTICLE INFO

Article history:
Received 13 March 2014
Received in revised form 24 April 2014
Accepted 22 May 2014
Available online 2 June 2014

Keywords:
Paramylon
Nanofiber
Electrospinning

ABSTRACT

(1 → 3)-β-D-Glucans of paramylon from *Euglena gracilis* were dissolved in concentrated formic acid and electrospinning was conducted using a newly designed setup. The diameter of the as-spun fibers ranged from 0.05 to 1 μm, and most of the fibers were straight and aligned parallel to two arbitrary fins (electrodes). By polarized optical microscopy, we determined that the anisotropic texture of the fibers was indicative of parallel alignment of the molecular chains to the fiber axis. The wide-angle X-ray scattering curve for the fibers showed amorphous halo scattering in spite of the high crystallinity of starting paramylon powder.

1. Introduction

(1 → 3)-β-D-Glucans are widespread in living organisms such as plants, fungi, yeasts, and bacteria (Clarke & Stone, 1960; Manners, Masson, & Patterson, 1973). Many studies have been conducted to describe their biological behavior such as immunomodulation and anti-tumoral activity, and the corresponding potential applications to the biomedical fields have been explored (Bohn & BeMiller, 1995; Kataoka, Muta, Yamazaki, & Takeshige, 2002; McIntire & Brant, 1998; Ooi & Liu, 2000; Vismar, Vestri, Frassanito, Barsanti, & Gualtieri, 2004; Wood, 1994).

To study the biological activities of paramylon, a carbohydrate found in *Euglena gracilis*, it is necessary to modify its stable triple-helical structure having approximately 90% crystallinity (Marchessault & Deslandes, 1979) into a more flexible one. 2,2,6,6-Tetramethylpiperidine-1-oxyl radical (TEMPO)-mediated oxidation is one of the most promising methods not only to increase paramylon solubility in water but also to produce its nanofibers (Tamura, 2012). However, chemical modification, i.e., the complete conversion of the C6 primary hydroxyl groups of paramylon into carboxylate groups, is inevitable (Tamura, Wada, & Isogai, 2009).

It would be preferable if we could prepare a paramylon solution without recurring to carboxylation. Shibakami, Tsubouchi, Nakamura, and Hayashi (2013) have developed a method based on the fibrillation of a bundle of nanofibers in a paramylon particle using NaOH aqueous solution, followed by the self-assembly of randomly coiled (1 → 3)-β-D-glucans into a triplex. However, their method comprised three complicated stages. In a previous paper (Kawahara & Koganemaru, 2006), we adopted formic acid as the solvent for paramylon and succeeded in the production of regenerated paramylon films even though the production of regenerated fibers via conventional wet spinning was difficult due to the decrease in the degrees of polymerization of (1 → 3)-β-D-glucans by hydrolysis reaction with formic acid.

2. Materials and methods

2.1. Materials

Spray-dried powder-like *E. gracilis* was furnished from Kanai Juyo Kogyo Co. Ltd., Japan. The powder was soaked in 0.25 N NaOH aqueous solution, shaken for 5 h, and settled for 1 day. The settlement was centrifuged and filtered. The obtained powder was neutralized with acetic acid and washed in water. Then, the paramylon powder was prepared. Other chemicals used were all of laboratory grade and were purchased from Wako Pure Chemical Industries Ltd., Japan.

2.2. Electrospinning

Paramylon powder was dissolved in 90% aqueous formic acid after constant stirring for at least 36 h, and then a 0.15 g/mL solution was prepared. Electrospinning was conducted at room temperature in ambient air with the setup shown in Fig. 1. The solution was loaded into a glass syringe equipped with a stainless steel needle,

* Corresponding author at: Corresponding author at: Division of Environmental Engineering Science, Gunma University, 1-5-1, Tenjin-cho, Kiryu 376-8515, Japan. Tel.: +81 277301491; fax: +81 277301491.
E-mail address: kawahara@gunma-u.ac.jp

http://dx.doi.org/10.1016/j.carbpol.2014.05.066
0144-8617/

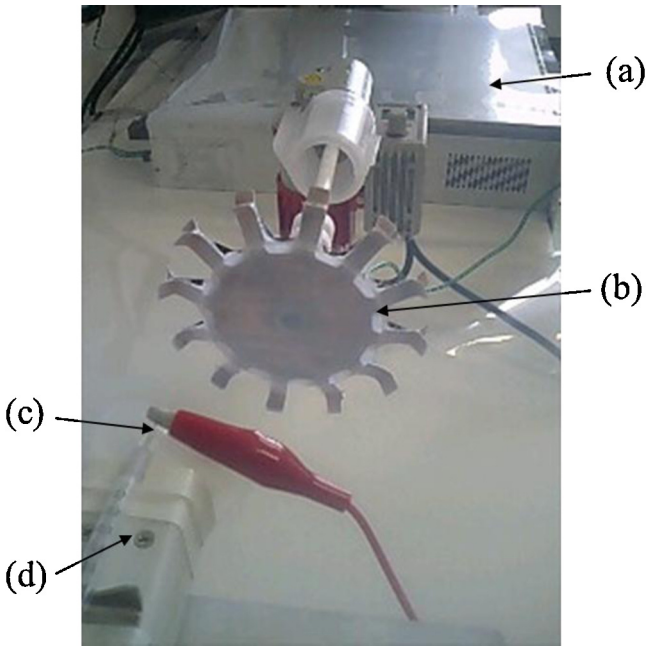

Fig. 1. Electrospinning setup: (a) high-voltage supply, (b) rotating collector, (c) needle, (d) syringe pump.

which was connected to a high-voltage supply. The solution was continuously supplied using a syringe pump at a rate of 10 μL/min through the needle. A voltage of 13 kV was applied for electrospinning. The distance between the needle tip and collector was approximately 10 cm. Li, Wang, and Xia (2004) demonstrated that electrospun fibers could be aligned parallel over long length scales during the spinning process by using a collector consisting of two conductive strips separated by a void gap of variable widths up to several centimeters. Thus, we designed a collector consisting of several fins similar to a pinwheel. The rotating speed of the wheel was 5 rpm. The electrospun fibers spanning across two arbitrary fins were collected and used for further measurements.

2.3. Relative viscosity

Paramylon solutions prepared at different stirring times (36–120 h) were cast on glass surfaces at room temperature, and then the regenerated films were obtained. Relative viscosity was measured at 30 °C with an Ostwald viscometer by dissolving the cast film of 0.1 g into dimethyl sulfoxide of 10 mL.

2.4. X-ray measurements

Wide-angle X-ray scattering (WAXD) profiles of the paramylon powder and electrospun fibers were obtained using a diffractometer (RINT2100FSL, Rigaku Co., Japan) and pinhole-collimated Cu*K*α X-rays. X-ray specimens were prepared by placing the powder or fibers into a thin quartz glass tube of 1.0 mm in diameter so that the volume of the specimen irradiated by the X-ray beam was kept approximately constant.

3. Results and discussion

The field emission-scanning electron microscopy (FE-SEM) images of the electrospun fibers are shown in Fig. 2. Many cracks perpendicular to the fiber axis are evident, especially in fibers thinner than 200 nm. These cracks were probably artifacts introduced by the electron beam irradiation attack during the FE-SEM observation. Most of the fibers were straight and parallel, even though

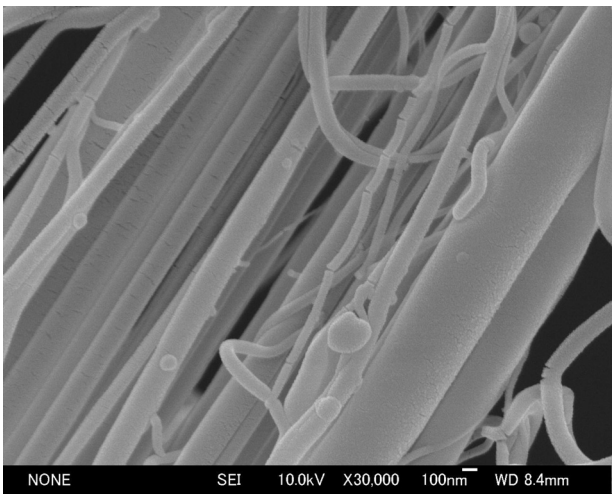

Fig. 2. Field emission-scanning electron microscopy (FE-SEM) images of the electrospun fibers observed without coating.

some of them were bent. With the geometrical configuration of the collector used in this study, when the fibers were collected across two arbitrary fins, they experienced a strong stretching force due to Coulomb interactions between the positive charges on the fibers and the negative imaginary charges on the grounded fins, i.e., electrodes (Li et al., 2004). Thus, the electrospun fibers tended to be aligned in parallel across the gap between the two fins. Fig. 3 shows the cumulative distribution of the fiber diameter for 50 random fibers. The distribution mode seems to be sigmoid. The average of the diameter was 192 ± 135 nm. Electrospinnability is greatly influenced by Berry number of the spinning solution (Baumgarten, 1971; Hager & Berry, 1982; Nasouri, Shoushtari, & Kaflou, 2012). Fig. 4 shows the dependence of Berry number on the stirring time at the preparation of the spinning solution. The intrinsic viscosity of paramylon could be calculated using the data for relative viscosity by applying the equation proposed by Solomon and Ciuta (1962). The fibers in Fig. 2 were electrospun using the paramylon solution at the stirring time of 48 h (Berry number = 18.5).

In the case of TEMPO-mediated oxidation, when the TEMPO/NaClO/$NaClO_2$ system was used, nanofibers with a diameter of approximately 1.98 nm could be produced, even though the conversion of the C6 primary hydroxyl groups of paramylon to carboxylate groups was inevitable (Tamura, 2012). The diameter of the triple-helical crystalline structure of (1 → 3)-β-D-glucans has been estimated to be approximately 1.56 nm (Chuah, Sarko, Deslandes, & Marchessault, 1983). Thus, the nanofiber obtained using TEMPO presumably consisted of a sequence of single

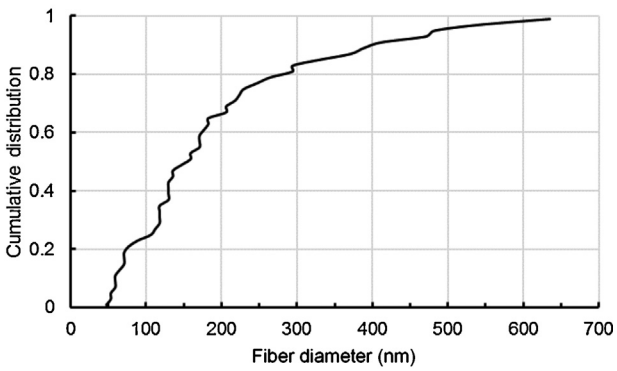

Fig. 3. Cumulative distribution of the fiber diameter.

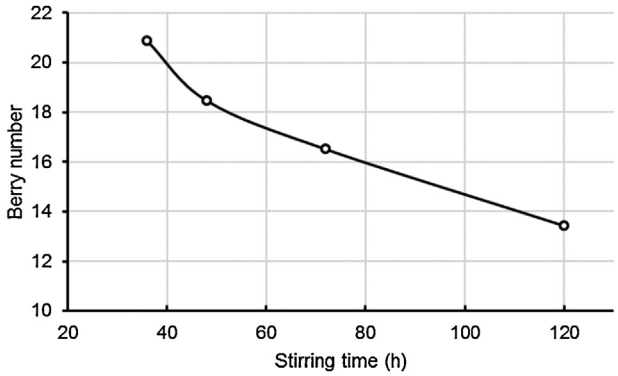

Fig. 4. Dependence of Berry number on the stirring time at the preparation of the spinning solution.

triple-helical chains of (1 → 3)-β-D-glucans, even though partially non-crystallized.

The polarized optical micrograph of the electrospun fibers is shown in Fig. 5. The anisotropic texture suggested that the alignment of the molecular chains was parallel to the fiber axis. The emergence of the anisotropic texture might indicate the formation of a mesophase in the spinning solution because the viscosity of the solution decreased with increasing stirring time during the preparation of the solutions (Kawahara & Koganemaru, 2003). Moreover, a relatively high concentration of solution (0.15 g/mL) was obtained in this study. However, the tensile strength of the cast films produced from the solution lowered with increasing stirring time (Kawahara & Koganemaru, 2003). Thus, the decrease in the viscosity seemed to be mainly due to the lowering of the molecular weight.

It is well known that electrospinning involves the rapid stretching of an electrical jet. Thus, an elongational stress would probably be applied to the molecules in solution. Therefore, (1 → 3)-β-D-glucan triple-helical chains were stretched and partially oriented along the fiber axis. We confirmed a similar behavior in the electrospinning of polydioxanone (Nakayama et al., 2007) and silk fibroin (Kawahara, Nakayama, Matsumura, Yoshioka, & Tsuji, 2008).

In Fig. 6, the WAXD curves of the paramylon powder and electrospun fibers are shown. Strong reflection peaks of the 1 0 0, 1 1 1, 2 1 0, and 1 2 1 planes of the paramylon crystallites were observed, while the curves of the electrospun fibers indicated amorphous halo scattering.

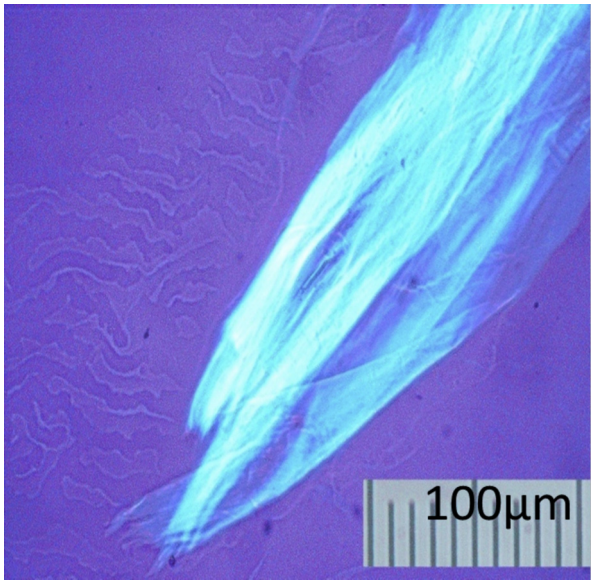

Fig. 5. Polarized optical micrograph of the bundle of electrospun fibers.

In the case of the nanofibers obtained using the TEMPO/NaClO/$NaClO_2$ system, the crystal reflections of the 1 0 0, 1 1 0, and 2 0 0 planes distinctly appeared in the WAXD curve (Tamura, 2012). Furthermore, the crystalline reflection peak from the 1 0 0 plane withstood, while other peaks from the 1 1 0 and 2 0 0 planes disappeared when the harsher TEMPO-mediated oxidation was initiated by increasing the amount of NaClO (Tamura et al., 2009). These results indicated that TEMPO-mediated oxidation could be categorized into a topochemical reaction. Therefore, nanofibers consisting of the sequence of single triple-helical (1 → 3)-β-D-glucans could be produced. On the contrary, when using formic acid as the solvent, dissolution accompanied by the hydrolysis of the (1 → 3)-β-D-glucans occurred randomly.

However, if the triple-helical structure is almost retained and the fibrillation is not so serious, the triple-helical structure might be restored through self-assembling. The water vapor annealing was effective in the enhancement of crystallinity for the electrospun PVA nanofibers (Yoshioka, Kawahara, Tsuji, & Schaper, 2011). Thus, the electrospun paramylon nanofibers were annealed in water vapor at 20 °C, 90%RH for 15 days, and the WAXD was measured. However, the WAXD pattern was hardly modified after

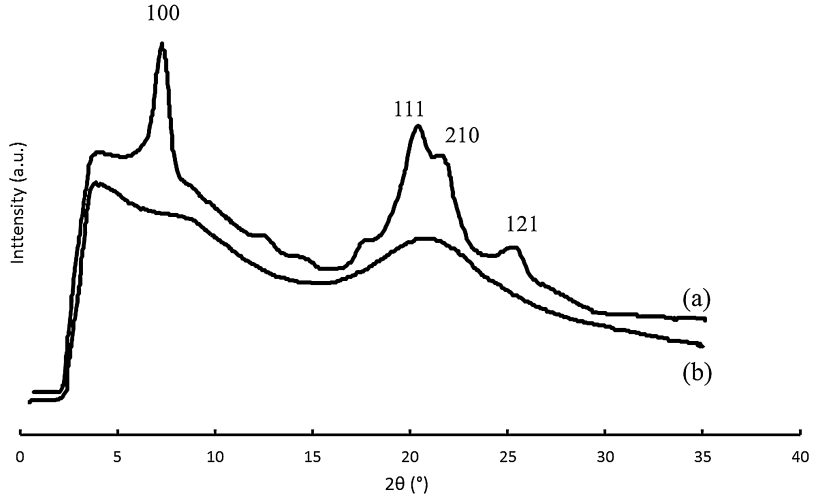

Fig. 6. Wide-angle X-ray scattering (WAXD) curves of (a) paramylon powder and (b) electrospun fibers.

the annealing. It seems that the triple-helical structure has been fibrillated to some extent. Therefore, the regenerated nanofibers became amorphous and fragile.

To enhance the accessibility of the (1 → 3)-β-D-glucans of paramylon to exploit its biological activities for further applications, the electrospinning method using formic acid is a convenient and promising candidate, since amorphous micropowder or dispersion of (1 → 3)-β-D-glucans could be easily obtained by combining ultrasonic grinding. In addition, the particle size of the powder, i.e., the fiber diameter, could be controlled by changing the spinning conditions such as applied voltage, concentration of solution, and winding speed.

4. Conclusions

(1 → 3)-β-D-Glucans of paramylon from *Euglena gracilis* were dissolved in concentrated formic acid and electrospinning was conducted using a newly designed setup. The diameter for the as-spun fibers ranged from 0.05 to 1 μm, and the WAXD curve of the fibers showed amorphous halo scattering, thus suggesting that the obtained nanofibers are too fragile to be used as reinforcing materials for composites. However, this brittle nature could be useful for the production of micropowders or dispersion of (1 → 3)-β-D-glucans by combining ultrasonic grinding.

Acknowledgment

The author would like to thank Prof. Takayuki Takarada for the FE-SEM observation.

References

Baumgarten, P. K. (1971). Electrostatic spinning of acrylic microfibers. *Journal of Colloid and Interface Science*, *36*, 71–79.

Bohn, J. A., & BeMiller, J. N. (1995). (1 → 3)-β-D-glucans as biological response modifiers: A review of structure-functional activity relationships. *Carbohydrate Polymer*, *28*, 3–14.

Chuah, C. T., Sarko, A., Deslandes, Y., & Marchessault, R. H. (1983). Packing analysis of carbohydrates and polysaccharides, Part 14. Triple-helical crystalline structure of curdlan and paramylon hydrates. *Macromolecules*, *16*, 1375–1382.

Clarke, A. E., & Stone, B. A. (1960). Structure of the paramylon from *Euglena gracilis*. *Biochimica et Biophysica Acta*, *44*, 161–163.

Hager, B. L., & Berry, G. C. (1982). Moderately concentrated solutions of polystyrene. I. Viscosity as a function of concentration, temperature, and molecular weight. *Journal of Polymer Science: Polymer Physics Edition*, *20*, 911–928.

Kataoka, K., Muta, T., Yamazaki, S., & Takeshige, K. (2002). Activation of macrophages by linear (1 → 3)-β-D-glucans—Implications for the recognition of fungi by innate immunity. *The Journal of Biological Chemistry*, *277*, 36825–36831.

Kawahara, Y., & Koganemaru, A. (2003). Development of a biodegradable film using paramylon prepared from *Euglena gracilis*. *Sen'i Gakkaishi*, *59*, 457–460.

Kawahara, Y., & Koganemaru, A. (2006). Development of novel film using paramylon prepared from *Euglena gracilis*. *Journal of Applied Polymer Science*, *102*, 3495–3497.

Kawahara, Y., Nakayama, A., Matsumura, N., Yoshioka, T., & Tsuji, M. (2008). Structure for electro-spun silk fibroin nanofibers. *Journal of Applied Polymer Science*, *107*, 3681–3684.

Li, D., Wang, Y., & Xia, Y. (2004). Electrospinning nanofibers as uniaxially aligned arrays and layer-by-layer stacked films. *Advanced Materials*, *16*, 361–366.

Manners, D. J., Masson, A. J., & Patterson, J. C. (1973). Structure of a β-(1 → 3)-D-glucan from yeast-cell walls. *The Biochemical Journal*, *135*, 19–30.

Marchessault, R. H., & Deslandes, Y. (1979). Fine structure of (1 → 3)-β-D-glucans: curdlan and paramylon. *Carbohydrate Polymer*, *75*, 231–242.

Mclntire, T. M., & Brant, D. A. (1998). Observations of the (1 → 3)-β-D-glucan linear triple helix to macrocycle interconversion using noncontact atomic force microscopy. *Journal of the American Chemical Society*, *120*, 6909–6919.

Nakayama, A., Kawahara, Y., Hayakawa, Y., Takahashi, R., Yoshioka, T., & Tsuji, M. (2007). Structural study on electrospun nanofibers of polydioxanone. *Sen'i Gakkaishi*, *63*, 230–234.

Nasori, K., Shoushtari, A. M., & Kaflou, A. (2012). Investigation of polyacrylonitrile electrospun nanofibers morphology as a function of polymer concentration, viscosity and berry number. *Micro & Nano Letters*, *7*, 423–426.

Ooi, V. E. C., & Liu, F. (2000). Immunomodulation and anti-cancer activity of polysaccharide–protein complexes. *Current Medicinal Chemistry*, *7*, 715–729.

Solomon, O. F., & Ciuta, I. Z. (1962). Determination de la viscosite intrinseque de solution de polymers par une simple determination de la viscosite. *Journal of Applied Polymer Science*, *6*, 683–686.

Shibakami, M., Tsubouchi, G., Nakamura, M., & Hayashi, M. (2013). Polysaccharide nanofiber made from euglenoid alga. *Carbohydrate Polymer*, *93*, 499–505.

Tamura, N. (2012). *Doctoral dissertation*. The University of Tokyo.

Tamura, N., Wada, M., & Isogai, A. (2009). TEMPO-mediated oxidation of (1 → 3)-β-D-glucans. *Carbohydrate Polymers*, *77*, 300–305.

Vismar, R., Vestri, S., Frassanito, A. M., Barsanti, L., & Gualtieri, P. (2004). Stress resistance induced by paramylon treatment in *Artemia* sp. *Journal of Applied Physiology*, *16*, 61–67.

Wood, P. J. (1994). Evaluation of oat bran as a soluble fiber source—Characterization of oat β-glucan and its effects on glycemic response. *Carbohydrate Polymer*, *25*, 331–336.

Yoshioka, T., Kawahara, Y., Tsuji, M., & Schaper, A. K. (2011). Structural modification of PVA nanofibers by water vapor annealing. *Sen'i Gakkaishi*, *67*, 138–140.